MOLECULAR PHYSICS, 1997, VOL. 92, NO. 1, 151–159

Density profiles and thermodynamics of rod-like particles between parallel walls

By Y. MAO[1], P. BLADON[2], H. N. W. LEKKERKERKER[3] and M. E. CATES[2]

[1] Cavendish Laboratory, Madingley Road, Cambridge, CB3 0HE, UK
[2] Department of Physics and Astronomy, University of Edinburgh, JCMB King's Buildings, Mayfield Road, Edinburgh EH9 3JZ, UK
[3] Van't Hoff Laboratory, University of Utrecht, Padualaan 8, 3584 Utrecht, The Netherlands

(*Received 24 February 1997; revised version accepted 9 April 1997*)

A study has been made of the density profile of mutually avoiding rod-like particles in the space between two parallel plates, held in equilibrium with a bulk phase of isotropic, semi-dilute rods, using a self-consistent integral equation which becomes exact as the rod aspect radio $L/D \to \infty$. Computer simulation investigations of finite aspect ratio systems also have been undertaken, and the extended Gibbs adsorption isotherm used to express the free energy (as a function of plate separation) in terms of an integral of the surface excess with respect to chemical potential. This allows thermodynamic properties, such as surface tension and the depletion force between plates, to be found. For $L/D \to \infty$, the results confirm both the thermodynamic consistency of the integral equation, and the accuracy of previous work on the depletion force (based on calculating only the contact density of rods at the walls). To extract thermodynamic data from the simulations, the same Gibbs isotherm method is very efficient, as it utilizes the statistics of the full density profile rather than just the contact density. Precise thermodynamic results for confined rod systems have been obtained from simulation for the first time. Those for $L/D = 10$ and 20 are shown to be quite close to the predictions for infinite aspect ratio.

1. Introduction

Calculations of the density profiles and thermodynamics of particles confined between parallel plates are of considerable interest in several contexts. These include studies of the solvation force [1], in which the confined particles are solvent molecules themselves, and of the depletion force [2], in which the particles are larger objects such as colloids or polymers, suspended in a solvent (now regarded as a continuum). The depletion force is central to issues of phase stability in colloidal systems [3, 4].

Several approximate theories have been used to calculate density profiles, including perturbation theory [5], homogeneous Percus–Yervick theory [6–8] and weighted density functional theory [9, 10]. Most of these offer access to thermodynamic information (surface tensions, forces between the plates) as well as density profiles themselves. Another important method is, of course, computer simulation [9, 11, 12]. However, many of these efforts have been restricted to the case of spherical particles.

In this paper, we consider the case of rod-like particles with hard core interactions. At first sight this problem appears difficult, and certainly the orientational variables make the calculations more involved than for spheres. But a much more striking difference is that, in the limit of long, thin rods (length L, diameter D, aspect ratio $L/D \to \infty$) there is *no need to make any approximation in the theory*. Instead, one can write down an exact integral equation for the density profile [13], which may be solved to whatever accuracy is required. This statement is the analogue, for confined rods, of Onsager's famous result concerning the bulk [14]. Onsager showed that, for an infinite aspect radio, the virial equation of state for rods can be truncated at second order, without approximation. The reason is that there is negligible probability of a sequence of rods in contact ever forming a loop. For rods between plates, this is still true, although mathematically the resulting simplification is less extreme. (Second-order perturbation theory is not valid here, because of loop closures involving the walls [15, 16].) Once the self-consistent integral equation has

been solved numerically, thermodynamic quantities such as the osmotic pressure and the force between the plates can be obtained, either from the contact density of rod ends at the walls using the pressure sum rule [15, 17], or from the adsorption isotherm presented below.

Because it can be solved to arbitrary accuracy for $L/D \to \infty$, a fluid of hard rods between plates offers an important testing ground for ideas about confined fluids generally. But of course available experimental systems do not lie in this limit. Tobacco mosaic virus, for instance, has an aspect ratio of about 17 [18]. To know whether the asymptotic results have any relevance to experimentally accessible systems, we must investigate the role of finite aspect ratio. This introduces several new effects, for example rods of finite aspect ratio could undergo layering close to the wall [19], causing changes in the contact density and thereby the depletion force. Below we report new computer simulation results for density profiles, the depletion potential and the surface tension. These show that for aspect ratios as small as 10 the asymptotic theory is surprisingly accurate.

The calculation of thermodynamic quantities by simulation requires care [20]. To find the force between plates, say, it is possible in principle to measure directly the pressures acting on the walls. This may be done using molecular dynamics [21], by measuring the contact density [15, 17], or by measuring the acceptance of virtual trial moves involving the box size [22]. We adopt a different way of calculating thermodynamic quantities, using the extended Gibbs equation [23, 24], as described below. This method depends only on measuring the density profile, rather than pressure directly, which can be done much more accurately in a simulation. The same approach may prove useful for other simulation problems where measuring the pressure is difficult, such as in lattice models. To our knowledge, this is the first time this technique has been used in computer simulation, although adsorption isotherms have been used to determine the location of prewetting transitions in simple fluids [25, 26].

The paper is organized as follows. In sections 2.1 and 2.2, we outline the calculation method for the infinite L/D limit, and the simulation technique for finite L/D. The results for the rod midpoint and endpoint density profiles, and also for the order parameter profile, are presented and compared in section 2.3. In section 3.1 we derive the extended Gibbs adsorption equation, which is then applied successively (in sections 3.2 and 3.3) to the integral equation and the simulation data. Thermodynamic and numerical consistency of the integral equation are explicitly demonstrated, and the first simulation data for the surface tension and depletion interaction of confined rod fluids are obtained. Section 4 contains a brief conclusion.

2. Density and order parameter profiles

2.1. *Infinite aspect radio*

For a system of spherocylinders with excluded volume interactions and aspect ratio $L/D \to \infty$, Onsager theory [14] allows us to write the thermodynamic grand potential as a functional of the one particle distribution function $n(\mathbf{r}, \Omega)$. Here n is the number density of rod *midpoints* at $\mathbf{r}$ with orientation $\Omega = (\theta, \phi)$. The minimization of the grand potential with respect to $n(\mathbf{r}, \Omega)$ gives an integral equation for the latter quantity [13]. The same self-consistent equation also can be obtained directly from a probabilistic argument [15]. An approximate solution for the single plate geometry can be found in [27]; however, as shown in [15], the equation can be solved numerically *without* further approximation.

For the general parallel plate geometry of interest here, the integral equation reads [15]

$$n_e(h, z_0, \Omega_1) = (n_b/2\pi)\exp\left((\pi c_b/2) + \int d\mathbf{r}_2\, d\Omega_2\, f_M(\mathbf{r}_1, \mathbf{r}_2, \Omega_1, \Omega_2) n_e(h, z_2, \Omega_2)\right) \quad \text{for } 0 < z_{0,1} < h,$$
$$= 0 \quad \text{otherwise.} \qquad (1)$$

Here h is the plate separation; n_b is the bulk number density and $c_b = n_b D L^2$ is the reduced bulk concentration; $\mathbf{r}_{1,2}$ denote the midpoint positions and $\Omega_{1,2} = (\phi_{1,2}, \theta_{1,2})$ denote the orientations of two given rods; $z_{0,1}$ and $z_{2,3}$ are the distances of the ends of these two rods measured, in units of L, from the lower plate (say) where the $z_{0,2}$ are chosen to be smaller than $z_{1,3}$. This geometry is illustrated in figure 1. The 'end density' $n_e(h, z, \Omega) = n(h, z + (\cos\theta)/2, \Omega)$ is defined as the number density of rods whose lower end is at z. Finally, f_M is the Mayer function which is equal to - 1 when the two molecules overlap with each other or with the plates, and zero otherwise.

Integral equation (1) was solved under the assumption that the uniaxial symmetry imparted by the parallel plate geometry is not spontaneously broken. This allows us to reduce the distribution function $n_e(h, z_0, \Omega_1)$ to $n_e(h, z_0, u)$, where $u = \cos\theta_1$. We expect this assumption to be valid for densities up to some transition point, in the vicinity of the bulk isotropic–nematic transition which arises at $c_b \simeq 4{\cdot}2$; rods of higher density would then adopt a biaxial arrangement near the surface. The stability analysis provided in [27] suggests that the uniaxial symmetry should be preserved for densities up to $c_b \approx 3{\cdot}5$ near a free surface. This criterion could of course depend now on the separation h (as well as the aspect ratio L/D if this is not large

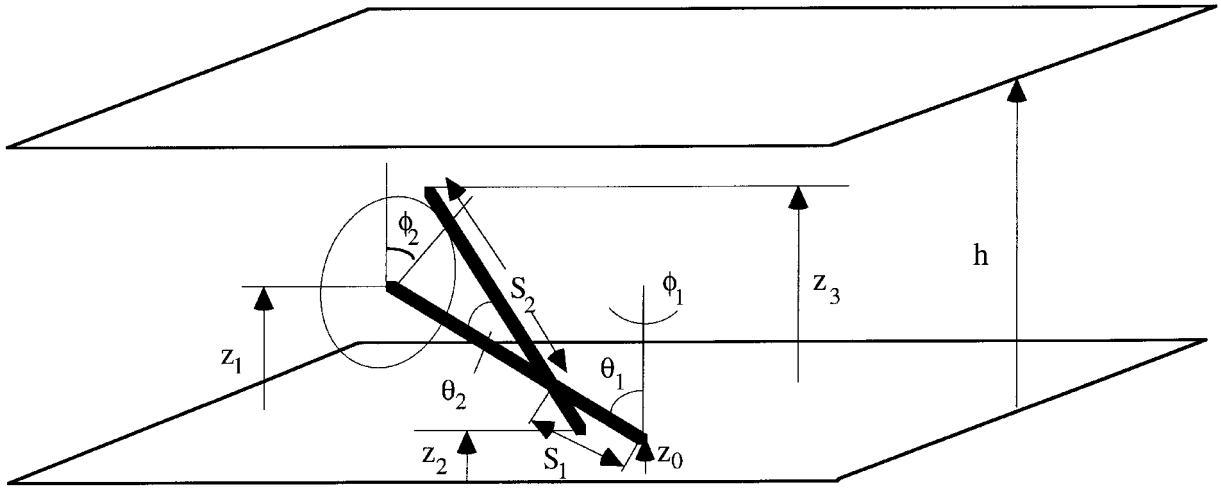

Figure 1. Geometry of the two-rod excluded volume calculation.

enough). However, the simulation results (see section 2.2) confirm the absence of biaxiality for densities up to $c_b = 2$.

The method for solving equation (1) numerically is non-trivial, and first requires rewriting the equation in a somewhat different form. The procedure is described in [15], so we do not give details here. The computation time required to solve equation (1) increases quite rapidly with concentration. For $c_b = 2$, about 5–10 hours of CPU time are required (on a DEC Alpha 600/5/266) to solve for the density profile $n_e(h, z_0, \Omega_1)$ with a particular separation h. The results found using this approach are discussed in section 2.3.

2.2. *Finite aspect ratio: computer simulation*

Grand canonical Monte Carlo simulations were used to investigate the effect of finite aspect ratio L/D. Spherocylinders, cylinders of length L, diameter D and with hemispherical end caps, were simulated in a parallel plate geometry at fixed activity $z = e^{\beta\mu}/\Lambda^3$ with μ the chemical potential and $\beta = 1/k_B T$ [28]. Simulations of a bulk system were used to determine the correspondence between the activity z and bulk density n_b. For the parallel plate systems, periodic boundary conditions were used in the x and y directions, and hard walls were placed perpendicular to the z direciton at each end of the simulation box. The plate separation h is defined as the maximum distance a particle midpoint can translate in the z direction. Thus, when $h = L$, a spherocylinder of length L will just fit in the box if its long axis is parallel to the z direction. In the x and y directions, the box size was $3 \times (L + D)$.

Using grand canonical simulations it was straightforward to measure the rod midpoint density profile, the rod end density profile, and the nematic and biaxial order parameter profiles. Rods of two aspect ratios were studied, $L/D = 10$ and $L/D = 20$, at two different reduced concentations $c_b = 1$ and $c_b = 2$. These, from simulations of the bulk, were found to require activities of $z = 0{\cdot}173$, $25{\cdot}0$ for the $L/D = 10$ system at $c_b = 1, 2$, respectively, and $z = 0{\cdot}0221$, $0{\cdot}651$ for the $L/D = 20$ system. All these systems were relatively small, for example, the simulation box for $L/D = 20$, $c_b = 2$ and $h/L = 1{\cdot}8$ contained about 700 particles. Despite this, we do not expect finite size effects to be large, as the number density between the plates was relatively low, and the systems were found always to have rotational symmetry around the z axis. The latter result (expected far from the bulk isotropic–nematic phase transition) shows that there is no surface-induced symmetry breaking which might lead to hysteresis effects.

2.3. *Results*

Figure 2 shows the normalized rod midpoint density, defined as $\tilde{n}(h, z) = \int n(h, z, u)\, d\Omega_1 / n_b$, at concentrations (*a*) $c_b = 1$ and (*b*) $c_b = 2$, as a function of the distance z from one plate. The plate separation is $h/L = 1{\cdot}8$. The smooth lines are found by solution of the integral equation (interpolated from a large dataset); the points with error bars are measured by simulation for aspect ratios $L/D = 10$, 20. It is clear that the wall effect penetrates the bulk to a distance of order L, and this effect decays slightly as density increases. For $c_b = 1$ the particle density between the plates is rather small; this accounts for the lack of any significant layering at the walls for rods of finite aspect ratio. (Note also that the density approaches the bulk density at the centre of the box.) In contrast, for the higher bulk density case ($c_b = 2$, figure 2(*b*)), there is significant layering at the walls arising from the finite aspect ratio of the rods. Layering

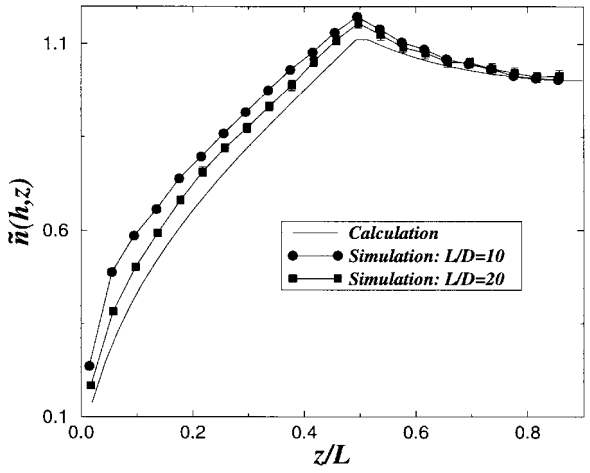

(*a*)

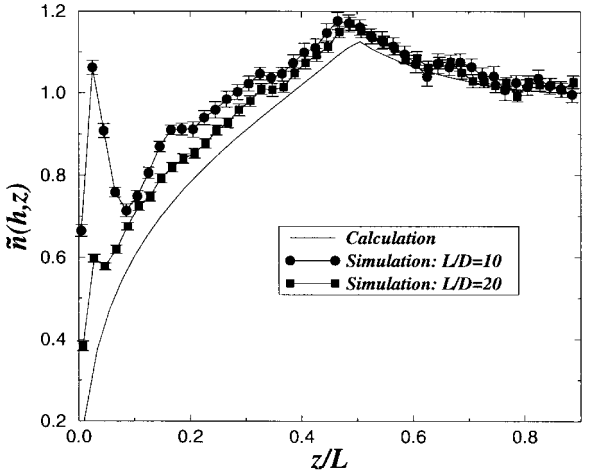

(*b*)

Figure 2. The normalized density of rod midpoints $\tilde{n}(h,z) = \int n(h,z,u)\,\mathrm{d}\Omega_1/n_\mathrm{b}$ as a function of distance from one plate z. The separation obeys $h/L = 1{\cdot}8$; reduced densities are (*a*) $c_\mathrm{b} = 1$, and (*b*) $c_\mathrm{b} = 2$. The smooth lines show the results of the integral equation; the points are simulation results for $L/D = 10$ and 20.

is, as expected, more pronounced in the $L/D = 10$ system. Nonetheless, the simulation results for $L/D = 10$, 20 show good convergence of the density towards the asymptotic theory for infinite aspect ratio.

The reduced density of the rod ends is defined as $\tilde{n}_\mathrm{e}(h,z) = \int (n_\mathrm{e}(h,z,u) + n_\mathrm{e}(h,z-u,u))\,\mathrm{d}\Omega_1/n_\mathrm{b}$. This is plotted, as a function of the distance z from one plate (figure 3) for $c_\mathrm{b} = 2$. Note that the reduced contact density $\tilde{n}_\mathrm{e}(h,0)$ gives the osmotic pressure on the plate (in units of $n_\mathrm{b}k_\mathrm{B}T$) and hence controls the depletion force. However, the fact that the osmotic pressure increases with decreasing aspect ratio does not imply the depletion force should behave in a similar way; the depletion force

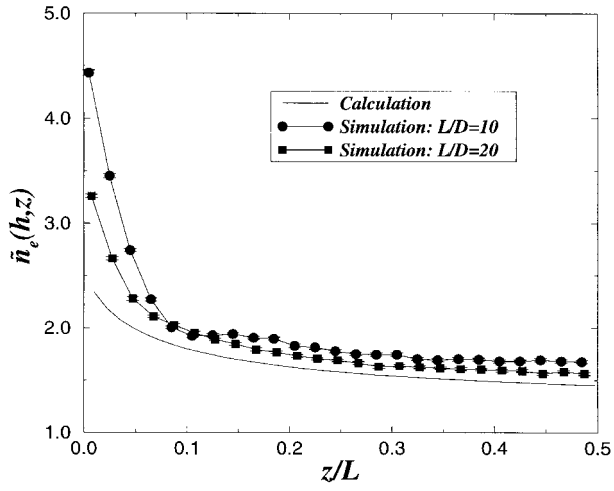

Figure 3. Normalized density of the rod ends $\tilde{n}_\mathrm{e}(h,z)$ as a function of distance from one plate z, for $c_\mathrm{b} = 2$. Here $h/L = 1$. The quantity $\tilde{n}_\mathrm{e}(h,0)$ gives the osmotic pressure in units of $n_\mathrm{b}k_\mathrm{B}T$.

results from the difference in osmotic pressure between the inside and outside surfaces of a plate. Again, for the rod end density there is satisfactory convergence of the simulation results towards the asymptotic calculation for the limit of long, thin rods.

The order parameter is defined locally by $Q(h,z) = \int n(h,z,u)P_2(u)\,\mathrm{d}\Omega_1/(n_\mathrm{b}\tilde{n}(h,z))$, which is the average over rod midpoints of the second Legendre polynomial. This is plotted in figure 4 as a function of z, for $h/L = 1{\cdot}8$. It appears that the order parameter profiles do not depend strongly on the rod density, nor on plate separation h. The negative value of Q indicates that the orientational distribution of rods is more pancake-like than cigar-shaped, as one expects from the influence of the parallel plate geometry. A rod lying very close to a

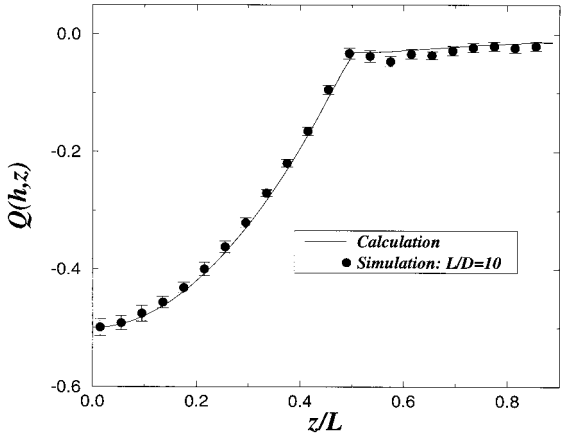

Figure 4. The order parameter $Q(h,z) = \int n(h,z,u)P_2(u)\,\mathrm{d}\Omega_1/(n_\mathrm{b}\tilde{n}(h,z))$ as a function of z, for $h/L = 1{\cdot}8$, and $c_\mathrm{b} = 2$.

wall must adopt a fully parallel alignment, so the order parameter reaches the limiting value of - 1/2 there. As the rod centre moves away from the wall, its order parameter returns towards the bulk value of zero. The simulation results show a very small deviation from those for infinite aspect ratio: at these densities, geometry, not interparticle interaction, is the significant factor in determining Q. Measurement of the biaxial order parameter, $B(z) = \langle 3/2(\sin^2\theta(z)\cos 2\phi(z))\rangle$ indicated that, at the concentrations studied, there was no biaxial order present in the simulated system. This confirms the assumption made in our numerical treatment of equation (1).

3. Surface thermodynamic properties

3.1. *An extended Gibbs adsorption equation*

To calculate surface thermodynamic quantities, such as the surface tension of a rod solution or the depletion interaction between plates, we start from a useful thermodynamic identity. This is a version of the Gibbs equation, and states that

$$\mathrm{d}\gamma(h) = -\Gamma(h)\,\mathrm{d}\mu. \tag{2}$$

Here $\gamma(h)$ is the surface excess free energy for *one of* a pair of parallel plates immersed in solution at separation h, and $\Gamma(h)$ the corresponding surface excess concentration of solute. In the limit $h \to \infty$, one has a surface contacting a semi-infinite fluid, and the conventional Gibbs treatment for the surface tension is recovered [29]; the usual surface tension is $\gamma = \gamma(\infty)$.

This result allows us to write the interaction energy between two flat plates as

$$W(h) = 2\gamma(h) - 2\gamma(\infty), \tag{3}$$

where

$$\gamma(h) = -\int_{-\infty}^{\mu} \Gamma(h)\,\mathrm{d}\mu. \tag{4}$$

This leads us to an extended form of the Gibbs adsorption equation

$$W(h) = -2\int_{-\infty}^{\mu} \left[\Gamma(h) - \Gamma(\infty)\right]\mathrm{d}\mu, \tag{5}$$

for which a more detailed derivation is presented in the appendix.

Equations (2)–(5) are central to this paper. They allow us to calculate surface thermodynamic properties such as $W(h)$, if we know the surface excess $\Gamma(h)$ as a function of μ.

Of course, alternatively the depletion potential $W(h)$ may be obtained by a direct integration of the depletion force

$$W(h) = \int_{h}^{\infty} f(h')\,\mathrm{d}h', \tag{6}$$

which requires knowledge of the contact density $n_e(h', 0)$ for all separations $h' > h$. Likewise, the surface tension γ of the hard rod fluid (with a single surface) is half the work required to separate two plates to infinity against the depletion force (thereby creating two new interfaces): $\gamma = -W(0)/2$.

There are two good reasons to reformulate these results in terms of the surface excess $\Gamma(h)$. First, the surface excess is a global property of the density distribution between the plates. Information from the whole density profile is used thereby to calculate the surface thermodynamic properties γ and $W(h)$. In contrast, the calculation via the depletion force method requires knowledge only of the density of rod ends at contact with the wall. The accuracy attainable from the adsorption equation therefore is likely to be much higher. This offers some advantages, even for the numerical solution of the exact integral equation. However, it becomes vital for the computer simulation results: calculation of the surface thermodynamics to comparable accuracy by a direct method would not have been practicable. Second, having two different routes to calculate $W(h)$ allows explicit demonstration that our integral equation (1) is thermodynamically consistent. Although this was never really in doubt, we cannot think of many other confined particle systems for which the free energy can be calculated, so precisely, in two quite separate ways. Viewed differently, the results offer a powerful check of our numerical treatment of equation (1): they are virtually identical to those obtained previously [15] from the contact density route.

3.2. *Infinite aspect ratio*

To calculate $W(h)$ from equation (1) via the surface excess, note first that $\Gamma(h)$ is defined from the end density profile $n_e(h, z, \Omega)$ as

$$\Gamma(h) = \int \mathrm{d}\Omega \int_0^{h/2} \mathrm{d}z \left(n_e(h, z, \Omega) - \frac{n_b}{2\pi} \right), \tag{7}$$

while the chemical potential μ is related to the bulk density n_b by [14]

$$\mu/k_B T = \ln n_b + n_b \pi D L^2/2. \tag{8}$$

Combining the above two equations, together with equation (5), we obtain

$$W(h) = 2k_B T \int_0^{n_b} \left[\Gamma(h) - \Gamma(\infty)\right] \left(\frac{1}{n_6} + \pi D L^2/2 \right) \mathrm{d}n_6. \tag{9}$$

The surface tension γ is then found as $\gamma = -W(0)/2$. In practice the surface excess $\Gamma(h)$ is easily evaluated numerically for any given n_b using equation (7). Repeating this procedure for a series of closely spaced n_b values allows the thermodynamic integration to be performed.

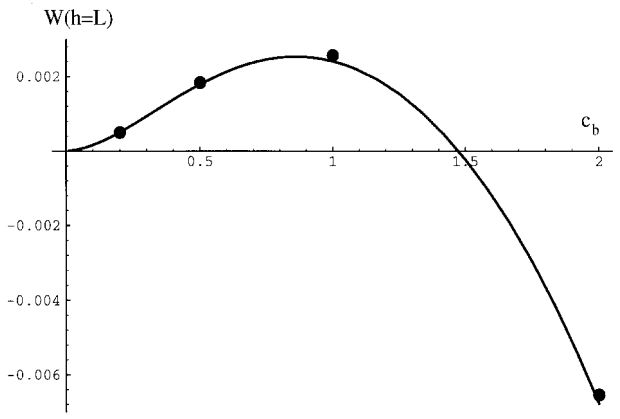

Figure 5. The numerically evaluated depletion potential for infinite aspect ratio, in the case of $h = L$: solid curve, from Gibbs equation; dots, from contact density by integration of the depletion force.

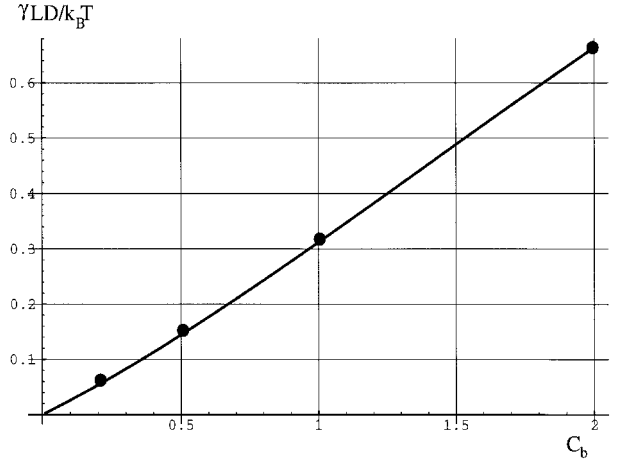

Figure 6. The numerically evaluated surface tension between a fluid of hard rods at infinite aspect ratio and a solid wall. This is plotted as a function of the reduced concentration c_b. Solid curve, from Gibbs equation; dots, from contact density by integration of the depletion force.

The only point of subtlety is to find $\Gamma(\infty)$, the surface excess for a wall contacting a semi-infinite solution. In practice, it is found that the rod density at the midpoint between the plates, $n_e(h, z = h/2, \Omega)$, approaches its $h \to \infty$ asymptote $(n_b/2\pi)$ for quite modest separations. Indeed, to within our numerical precision, we found that an accurate evaluation of $\Gamma(\infty)$ for each n_b could be achieved for a fixed plate separation $h = 3L$ at all densities up to $c_b = 2$. (For much higher densities, a larger h might be required.)

The results found in this way for the depletion potential $W(h)$ (as a function of c_b for a particular separation $h = L$) are shown in figure 5. For comparison, we also show the results for selected c_b (from [15]), found by the direct integration of the contact density, without the use of the extended Gibbs equation. The agreement clearly is excellent. The surface tension γ is plotted similarly as a function of c_b in figure 6. At low densities, the surface tension approaches the osmotic pressure $n_b k_B T$ times the orientationally average excluded volume $DL^2/4$ due to the wall; the slope of the curve therefore tends to 0·25. Agreement with the results of directly integrating the contact density again are very good overall.

3.3. *Finite aspect ratio*

To obtain $W(h)$ from the simulated density profiles, we proceed by rewriting the equation for the surface excess, equation (7), explicitly as the difference between the number of particles per unit area in the confined system and that in an equivalent bulk system of the same size:

$$\Gamma(h) = \frac{1}{2A}\left(N^{\text{wall}}(h) - N^{\text{bulk}}(h)\right). \tag{10}$$

Here $N^{\text{wall}}(h)$ is the ensemble average number of particles in the simulation box of the system between plates, and A is the cross-sectional area of the box; $N^{\text{bulk}}(h) \equiv n_b h$ is the corresponding quantity for the same volume within a bulk system. Both of these quantities can be measured *extremely* accurately in a simulation.

In terms of the activity z, the depletion potential is given by

$$W(h) = 2k_B T \int_0^{z_b} \left\{ \frac{1}{2A}\left[N^{\text{wall}}(h) - N^{\text{bulk}}(h)\right] - \Gamma(\infty) \right\} \times \frac{dz}{z}, \tag{11}$$

where z_b is the activity corresponding to bulk density n_b, and the identity $dz/z = \beta\, d\mu$ has been used. Just as before, the integration to obtain $W(h)$ is straightforward except for the term in $\Gamma(\infty)$. This term determines the surface tension, but it can be viewed also as a constant which ensures that $W(h)$ asymptotes to zero at large separations. Accordingly we choose to write

$$W(h) - W(0) \equiv \tilde{W}(h) = \tilde{W}^{\text{wall}} - \tilde{W}^{\text{bulk}}, \tag{12}$$

where

$$\tilde{W}^{\text{wall}}(h) = \frac{k_B T}{A} \int_0^{z_b} N^{\text{wall}}(h) \frac{dz}{z}, \tag{13}$$

$$\tilde{W}^{\text{bulk}}(h) = \frac{k_B T}{A} h \int_0^{z_b} n_b \frac{dz}{z}, \tag{14}$$

thereby separating $\tilde{W}$ into contributions from the confined system and the equivalent bulk.

For each of the aspect ratios studied (L/D = 10, 20) and each plate separation, a series of 18 simulations was performed, decreasing z by a factor of two each time from an initial value z_b (as given in section 2.2). The non-interacting limit $N^{\text{wall}} \propto z$ was attained with small z in all cases. The change of variable $q = z^{1/4}$ was made to facilitate integration of the data, and the resulting set of points interpolated with a cubic spline. By this procedure, an accurate determination of $\tilde{W}^{\text{wall}}$ was obtained.

The corresponding integral, equation (14), for $\tilde{W}^{\text{bulk}}$ can in principle be evaluated the same way, using additional simulations on bulk systems (e.g., with periodic boundary conditions) to accurately determine $n_b(z)$. The result for $\tilde{W} = \tilde{W}^{\text{wall}} - \tilde{W}^{\text{bulk}}$ should asymptote to a constant, $\tilde{W}(\infty) = 2\gamma$, for large plate separations (in practice, this means $h/L > 3$). However it was found that, using this method to calculate $\tilde{W}^{\text{bulk}}$, the resultant $\tilde{W}(h)$ had a slight non-zero slope for large h/L. This problem arises because for large h, N^{wall} asymptotes to $n_b h + \Gamma(\infty)$; this includes a linear term which should be cancelled precisely by the N^{bulk} contribution. However, tiny errors in the respective coefficients of h (that is, small differences in these two independent estimates of n_b) will lead to a systematic non-zero slope of $\tilde{W}(h)$ for large h. To overcome this problem, $\tilde{W}^{\text{bulk}}$ was extracted instead directly from the large h region of $\tilde{W}^{\text{wall}}(h)$ by fitting a straight line to the last five points (h/L in the range 2·5–4). The intercept of this straight line then gives the surface tension.

Figure 7 shows a comparison of the calculated and simulated depletion potentials $W(h)$ for c_b = 1. There is, once again, good convergence of the finite aspect ratio results towards the asymptotic curve. These data

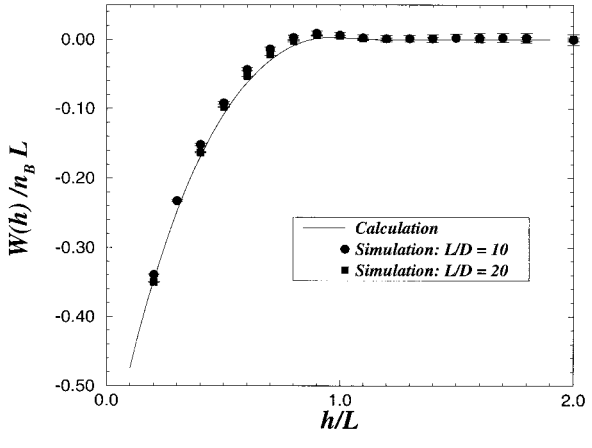

Figure 7. The depletion potential of the two plates $W(h)$ versus h/L for rods of aspect ratio L/D = 10, and 20. The finite aspect ratio of the rods gives a very slight enhancement to the potential barrier.

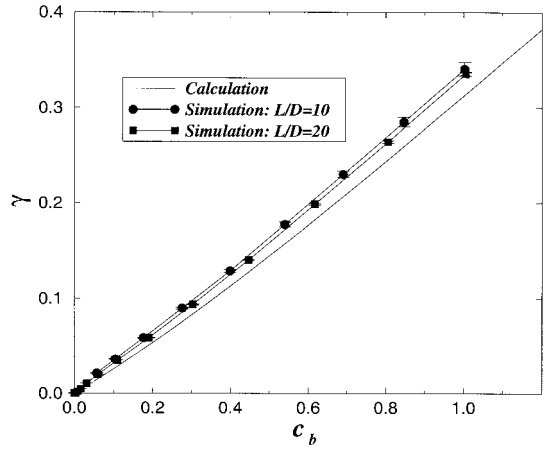

Figure 8. The surface tension, in units of $k_B T/LD$, between a fluid of hard rods and a solid wall, as a function of the reduced concentration.

confirm not only the well known primary minimum in the depletion potential [30], but also the presence of a finite (though very small) barrier. The existence of a barrier was predicted first using perturbation theory; on dimensional grounds [16] the barrier height should be of order $W_{\max} = \alpha(c_b) k_B T/(LD)$, where α is of order unity for $c_b \simeq 1$. In other words, *a priori* one would expect the barrier height to be clearly visible on the reduced plot shown in figure 7. The perturbative prediction is in fact $\alpha(1) = 0{\cdot}0221$, whereas the integral equation gives a yet smaller value, $\alpha(1) = 0{\cdot}0025$.

The reasons for the extremely small value of α are understood only partially [15]. However, presumably they involve some degree of cancellation by competing contributions, which could be upset easily by finite aspect ratio corrections. Therefore it is very important to check whether or not the barrier is significant for realistic L/D. (The presence of a large barrier would have very marked effects on issues of colloidal stability, as discussed in [16].) In fact, although we find a barrier height that is systematically higher for the finite aspect ratios studied, it is not much (a factor of about two for c_b = 1). Whereas a detailed analysis of the barrier height is precluded by the errors, we note that the simulation data are actually of remarkable accuracy: we are resolving features on the scale of $\alpha = 10^{-2}$ even though the fundamental scale of the interaction potential should be $\alpha \simeq 1$. Such an accuracy might be much harder to obtain if the extended Gibbs equation were not employed. Overall, however, the effect of finite rod aspect ratios on the depletion potential is rather weak.

Finally, figure 8 shows the surface tension of the hard rod fluid as a function of c_b (results from figure 6 are replotted for comparison). Again the effect of finite

aspect ratio is fairly weak; the asymptotic theory is good to within about 10% for $L/D = 10$.

4. Conclusion

We have presented rod end and midpoint density profiles, and order parameter profiles, for hard rod fluids between parallel plates. Results were obtained both from a self-consistent integral equation, exact in the limit $L/D \to \infty$, and from computer simulation for $L/D = 10$, 20. The latter results show that the stated aspect ratios are already quite close to the asymptotic limit, apart from some layering observed for high bulk densities ($c_b = 2$) in the case $L/D = 10$.

We then obtained an extended Gibbs adsorption equation $dW(h) = -2[\Gamma(h) - \Gamma(\infty)]d\mu$, where $\Gamma(h)$ is the surface excess for a single plate separated by h from another, and $W(h)$ is the depletion interaction between plates. (From this follows the usual surface tension via $\gamma = -W(0)/2$.) Methods based on integrating this equation were argued to have significant advantages, in accurately evaluating the free energy of confined rod fluids, over traditional methods based on the pressure sum rule (which involves only the contact density at the walls). This applies especially to computer simulations, where computational errors can be reduced substantially by using information from the full density profile. The technique may be suited equally to other systems in which the pressure is difficult to measure; these include complex molecules with hard interactions, and also lattice systems.

Using these methods, the effects of the finite rod aspect ratio on both the depletion potential and the surface tension were examined. Broadly speaking, the results for infinite aspect ratio remain qualitatively valid for the full range of parameters ($L/D = 10$, 20, $c_b = 1$, 2) studied here, and at these densities are likely to be correct to within a few per cent for $L/D > 20$. One exception to this lies in the height of the depletion barrier, which is increased by a factor of 2 or 3 at $c_b = 1$. However, this barrier remains very small (of order 10^{-2} in dimensionless units).

Finally, because of the accuracy of the results obtainable, we believe that the hard rod fluid merits further attention as a testing ground for more general ideas concerning the behaviour of fluids in confined geometries. Of course, it merits attention also in its own right. For example, the depletion force profiles we have derived should be measurable experimentally, using (say) TMV ($L/D \simeq 17$) in a force machine apparatus [31].

Y.M. is grateful to Trinity College, Cambridge for a Research Studentship. This collaboration was funded in part by the Colloid Technology Programme.

Appendix

Extended Gibbs isotherm

For intermediate separations h, the extended Gibbs adsorption equation can be derived as follows. The appropriate thermodynamic potential to describe a system of parallel plates of unit area in a rod solution is the grand potential

$$\Psi = F - \mu N, \tag{A 1}$$

where F is the Helmholtz free energy and N the number of particles in the system. For constant temperature and volume we have:

$$d\Psi = -f\,dh - N\,d\mu, \tag{A 2}$$

where f is the depletion force. From equation (A 2), it follows that

$$\left(\frac{\partial f}{\partial \mu}\right)_h = \left(\frac{\partial N}{\partial h}\right)_\mu, \tag{A 3}$$

but on the other hand we write

$$f = -\left(\frac{\partial W}{\partial h}\right)_\mu,$$

so a substitution gives

$$-\left(\frac{\partial}{\partial h}\left(\frac{\partial W}{\partial \mu}\right)_h\right)_\mu = \left(\frac{\partial N}{\partial h}\right)_\mu. \tag{A 4}$$

Integration of this equation with respect to h leads to

$$-\left(\frac{\partial W}{\partial \mu}\right)_h = N(h) - N(\infty). \tag{A 5}$$

For plates of unit area, we have $N(h) - N(\infty) = 2[\Gamma(h) - \Gamma(\infty)]$, where the surface excess $\Gamma(h)$ is given by equation (7),

$$dW = -2[\Gamma(h) - \Gamma(\infty)]\,d\mu, \tag{A 6}$$

which is the extension of the Gibbs adsorption equation to the case of two surfaces with finite separation. The integration of this gives

$$W(h) = -2\int_{-\infty}^{\mu}[\Gamma(h) - \Gamma(\infty)]\,d\mu. \tag{A 7}$$

References

[1] Grimson, M. J., and Richmond, P., 1980, *J. chem. Soc. Faraday Trans* ii, **76,** 1478; Grimson, M. J., and Rickayzen, G., 1981, *Molec. Phys.*, **42,** 767.

[2] See, e.g., Fleer, G. J., Cohen Stuart, M. A., Scheutjens, J. M. H. M., Cosgove, T., and Vincent, B., 1993, *Polymers at Interfaces* (London: Chapman & Hall).

[3] Poon, W. C. K., and Pusey, P. N., 1995, *Observation, Prediction and Simulation of Phase Transitions in Complex Fluid*, edited by M. Baus, L. F. Rull and J.-P. Ryckaert (Dordrecht: Kluwer).

[4] Vroege, G. J., and Lekkerkerker, H. N. W., 1992, *Rep. progr. Phys.*, **55,** 1241.
[5] Glandt, E. D., 1980, *J. Colloid Interface Sci.*, **77,** 512.
[6] Lebowitz, J. L., 1964, *Phys. Rev.*, **133,** 895.
[7] Attard, P., 1989, *J. chem. Phys.*, **91,** 3083.
[8] Henderson, D., 1988, *J. Colloid Interface Sci.*, **121,** 486.
[9] Hansen, J. P., and McDonald, I. R., 1986, *Theory of Simple Liquids* (London: Academic Press).
[10] McQuarrie, D. A., 1976, *Statistical Mechanics* (New York: Harper and Row).
[11] Van Megen, W., and Snook, I. K., 1979, *J. Chem. Soc. Faraday Trans* ii, **75,** 1095; Lane, J. E., and Spurling, T. H., 1979, *Chem. Phys. Lett.*, **67,** 107.
[12] Frenkel, D., 1987, *Molec. Phys.*, **60,** 1; Frenkel, D., and Mulder, B. M., 1985, *Molec. Phys.*, **55,** 1171.
[13] Poniewierski, A., and Holyst, R., 1988, *Phys. Rev.* A, **38,** 3721.
[14] Onsager, L., 1949, *Ann. NY Acad. Sci.*, **51,** 627.
[15] Mao, Y., Cates, M. E., and Lekkerkerker, H. N. W., 1997, *J. chem. Phys.*, **106,** 3721.
[16] Mao, Y., Cates, M. E., and Lekkerkerker, H. N. W., 1995, *Phys. Rev. Lett.*, **75,** 4548.
[17] Holyst, R., 1989, *Molec. Phys.*, **68,** 391.
[18] Fraden, S., 1995, *Observation, Prediction and Simulation of Phase Transitions in Complex Fluids*, edited by M. Baus, L. F. Rull and J.-P. Ryckaert (Dordrecht: Kluwer).
[19] Telo Da Gama, M., 1995, *Observation, Prediction and Simulation of Phase Transitions in Complex Fluids*, edited by M. Baus, L. F. Rull and J.-P. Ryckaert (Dordrecht: Kluwer).
[20] Frenkel, D., 1995, *Observation, Prediction and Simulation of Phase Transitions in Complex Fluids*, edited by M. Baus, L. F. Rull and J.-P. Ryckaert (Dordrecht: Kluwer).
[21] Rebertus, D. W., and Sando, K. M., 1997, *J. chem. Phys.*, **67,** 2587.
[22] Eppenga, R., and Frenkel, D., 1984, *Molec. Phys.*, **52,** 1303.
[23] Hall, D. G., 1972, *J. chem. Soc. Faraday Trans* ii, **68,** 2169; Ash, S. G., Everett, D. H., and Radke, C., 1973, *J. chem. Soc. Faraday Trans* ii, **69,** 1256.
[24] Evans, R., and Marconi, U. M. B., 1987, *J. chem. Phys.*, **86,** 7138.
[25] Finn, J. E., and Monson, P. A., 1989, *Phys. Rev.* A., **39,** 6403.
[26] Peterson, B. K., and Gubbins, K. E., 1987, *Molec. Phys.*, **62,** 215.
[27] Poniewierski, A., 1993, *Phys. Rev.* E, **47,** 3396.
[28] Allen, M. P., and Tildesley, D. J., 1986, *Computer Simulation of Liquids* (Oxford: Clarendon Press).
[29] Rowlinson, J. S., and Widom, B., 1982, *Molecular Theory of Capillarity* (Oxford: Clarendon press), pp. 34–46.
[30] Asakura, S., and Oosawa, F., 1954, *J. chem. Phys.*, **22,** 1255; 1958, *J. Polymer Sci.*, **33,** 183.
[31] Israelachvili, J. N., 1992, *Intermolecular and Surface Forces*, 2nd Edn (London: Academic Press).